Available online at www.sciencedirect.com
ScienceDirect
Chemical Physics 331 (2006) 142–158
Chemical Physics
www.elsevier.com/locate/chemphys

Solvation of monovalent anions in acetonitrile and *N*,*N*-dimethylformamide: Parameterization of the IEF-PCM model

Elvis S. Böes [1], Paolo R. Livotto, Hubert Stassen [*,2]

Grupo de Química Teórica, Instituto de Química, Universidade Federal do Rio Grande do Sul, Av. Bento Gonçalves 9500, 91540-000 Porto Alegre-RS, Brazil

Received 13 April 2006; accepted 28 August 2006
Available online 18 October 2006

Abstract

The present work reports the parameterization of the polarizable continuum model for predicting the free energies of solvation for monovalent anions in acetonitrile and *N*,*N*-dimethylformamide. The parameterization of the model for acetonitrile employed the experimental free energies of solvation for a set of 12 charged solutes, containing H, C, N, O, S, F, Cl, Br, and I atoms. For the *N*,*N*-dimethylformamide solutions, experimental solvation free energies for 11 monovalent anions were used. A mean absolute error of 0.7 kcal/mol in the solvation free energies has been achieved for the 12 anions in acetonitrile, whereas the mean absolute error for the 11 anions corresponds to 0.5 kcal/mol in *N*,*N*-dimethylformamide. These results indicate that the polarizable continuum model is a suitable methodology for the study of thermodynamic effects in solutions of monovalent anions in both solvents.

Keywords: Free energy of solvation; Polarizable continuum model; CH_3CN; DMF

1. Introduction

The influence of the solvent on chemical phenomena has been observed for a long time and it has received the attention of researchers from both, experimental and theoretical fields related with chemistry. For example, it is well known that the rate of a chemical reaction can change by many powers of 10 only by changing the reaction medium [1]. In addition to its impact on reactivity, the solvent also can modify the molecular structures and charge distributions as revealed by vibrational and electronic spectroscopy on molecules in solution [2]. Many of these phenomena have been explained by qualitative concepts or by empirical strategies based on the parameterization of experimental data for physical and chemical properties of solvents and the present intermolecular forces [3].

Using the intermolecular interactions that act between the solvent molecules and solutes, one may classify solvents into three categories [4]. Depending on the ability of solvent molecules to form hydrogen bonds with the solute molecules, we can classify the solvents as apolar aprotic, polar protic and aprotic. Apolar aprotic solvents have dielectric constants lower than 15, and possess low dipole moments. In this group, we include hydrocarbons, their halogen derivatives, tertiary amines, and carbon disulfide. Polar protic solvents posses molecular structures with hydrogen atoms bound to electronegative elements such as oxygen, and are hydrogen bond donors. These solvents are characterized by dielectric constants usually larger than 15. Good examples of protic solvents are water, ammonia, alcohols, carboxylic acids, amines and some amides. Protic solvents are usually good anion solvators due to their hydrogen bonding ability.

In this work, we are particularly interested in solvents belonging to the third group of solvent classes, namely the polar aprotic, or the non-hydrogen bond donor sol-

* Corresponding author. Tel.: +55 51 3316 7197; fax: +55 51 3316 7304.
E-mail addresses: elvis@iq.ufrgs.br (E.S. Böes), livotto@iq.ufrgs.br (P.R. Livotto), gullit@iq.ufrgs.br (H. Stassen).
[1] E.S.B. acknowledges a scholarship from the Brazilian agency CAPES.
[2] H.S. acknowledges a grant from Brazilian agency CNPq (309211/2003–2004).

0301-0104/$ - see front matter © 2006 Elsevier B.V. All rights reserved.
doi:10.1016/j.chemphys.2006.08.028

vents. These solvents usually possess dielectric constants larger than 30, and their molecules exhibit dipole moments larger than 2.0*D*. Additionally, the presence of lone electron pairs makes them good cation solvators. The main solvents of this group are dimethylsulfoxide, nitromethane, *N*,*N*-dimethylformamide (DMF), acetonitrile (AN), acetone, nitrobenzene, cyclic ureas, hexamethylphosphoric triamide, sulfolane, among others.

The relevance of studying the solvation of ionic species in solvents with these characteristics is related to experimental evidences that some S_N2 type reactions are remarkably accelerated in polar aprotic solvents [5] when compared to protic solvents. A possible explanation for these observations is the weaker ability of aprotic solvents to solvate anions that consequently behave more freely to react with the saturated carbon atom [6] than in protic solvents, in which anions are hydrogen bound to the solvent molecules. Many other chemical reactions involve mechanisms via ions or charged transition states. Thus, the observation that anion solvation is correlated to the rate constants of chemical reactions motivated us to initiate a theoretical study modeling anion solvation in polar aprotic solvents. From this kind of studies, important principles can be established for the selection of solvents suitable for supporting specific chemical reactions and processes [4].

Due the development of new theoretical methodologies and computational tools in recent years, it became feasible to model physical and chemical phenomena in solution. Among the most important methodologies, we mention classical force field approaches such as Monte Carlo and Molecular Dynamics simulations [7]. Another promising concept is represented by the supermolecule approach in which the solute and the solvent molecules are explicitly treated in quantum mechanical calculations [8]. If quantitative yields are required, the supermolecule approach becomes computationally very expensive, but, nevertheless, there is an increasing trend in the use of such methods as more powerful computational tools become available. Finally, we mention methodologies based on continuum models for the solvent. In this approach, the solute is explicitly treated by quantum chemical methods, whereas the solvent surrounding the solute is considered as a continuous medium endowed with physical properties related to its electrostatic behavior. These methods have been widely adopted in recent years, especially in the description of the energetic characteristics of solvation [9–11]. In addition, models based on combinations of the cited approaches have been proposed [12–16].

In this work, we draw attention to a specific continuum model called the polarizable continuum model (PCM). This model presents good accuracy, reliability, adaptability, and a reduced computational effort in describing solvent effects [17–19]. The PCM simulates the solvation process by embedding the solute inside a cavity surrounded by the solvent which is represented by an infinite continuous bath characterized by its bulk physical parameters such as the dielectric constant. The solute is represented by an accurate charge distribution obtained from quantum mechanical calculation. According to this model, the solute's charge distribution polarizes the surrounding dielectric medium inducing apparent charges on the surface of the solute cavity. These charges generate a reaction field, which is introduced into the quantum mechanical Hamiltonian for the solute by a perturbation operator. This operator induces a rearrangement of the charge distribution of the solute. The new charge distribution induces a new reaction field and so on, leading to an iterative procedure aborted when self-consistency is reached. We skip over the mathematical details of this formalism, and address the reader to Refs. [9,10,20–23] for detailed reviews concerning the PCM.

The construction of the cavity for the solute is one of the crucial steps in the procedures of the PCM. Defining the solute/solvent boundary, the solute's cavity is carefully built according to the molecular shape of the solute with the cavity size depending on the atomic radii of the solute molecule and on the solvent under study [24]. Thus, for studying the solvation process, the PCM needs to be parameterized with the suitable solute's cavity in the solvent under consideration. This parameterization is usually undertaken by adapting a scaling factor to the solute's atomic radii. Generally, this scaling factor is chosen by maximizing the agreement between experimental data and computed values of some property for a representative group of solutes in a given solvent. Several parameterizations of the PCM, which make directly use of atomic radii and a suitable scaling factor, are described in the literature for the solvation processes of neutral molecules in water [16] and organic solvents such as chloroform [24], carbon tetrachloride [25], and octanol [26].

Less attention has been devoted to the application of PCM to solvation of charged molecules. We cite the parameterization for the solvation of ionic solutes in water [27,28] and, more recently, in dimethylsulfoxide [29]. In this work, we present the parameterization of the PCM for the solvation of anions in two polar aprotic solvents, namely AN and DMF. These two solvents are of great importance as indicated by their widespread use in several operations of chemistry [30].

2. Parameterization procedures

In our study on anion solvation in acetonitrile and *N*,*N*-dimethylformamide, we firstly chose a set of anions to be included in this work. Initially, we selected all the anions for which experimental values for the free energy of transfer from water to AN and DMF are available [31,32]. We combined these data with the aqueous free energy of solvation from Pliego and Riveros [33] for F^-, Cl^-, Br^-, I^-, N_3^-, CN^- and $CH_3CO_2^-$, the hydration free energy data for I_3^- and SCN^- anions from Marcus [34], the NO_3^- anion hydration free energy from Florian and Warshel [35], and the aqueous solvation free energy value for the picrate (Pic^-) anion from Kusakabe and Arai [36]. For the ClO_4^- anion,

we have taken the solvation free energy in water from the work of Abraham and Liszi [37]. These experimental data are all corrected, when necessary, to the recently obtained standard value for the experimental solvation free energy for the proton in water, $\Delta G^{\circ}_{\mathrm{solv}}(\mathrm{H}^{+}) = -264$ kcal/mol [38], corresponding to the process of transfer of the proton from ideal gas at 1 atm to ideal diluted solution at 1 mol/l.

The experimental free energies of solvation for the anions were taken from the references just described and were converted, when needed, to a consistent standard state for discussing the Gibbs energy of transfer in accordance to Ben-Naim describing the process of transfer for 1 mol of solute per liter of ideal gas to 1 mol/l of ideal solution in the solvent [39]. In this standard state, used throughout the remainder of the article, the Gibbs free energy of hydration for the proton becomes $\Delta G^{*}_{\mathrm{solv}}(\mathrm{H}^{+}) = -265.9$ kcal/mol, where the relation

$$\Delta G^{*}_{\mathrm{solv}} = \Delta G^{\circ}_{\mathrm{solv}} - RT\ln(\widetilde{R}T) = \Delta G^{\circ}_{\mathrm{solv}} - 1.9\ \mathrm{kcal/mol} \quad (1)$$

is used to convert the energies between the two standard states [33,40]. In Eq. (1), $\widetilde{R}$ represents the converted gas constant, $\widetilde{R} = 0.08206$ atm l/K mol.

The Gibbs energy of hydration for the ClO_4^- anion given by Abraham and Liszi [37] refers to the transfer of the solute between the ideal gas phase at 1 atm and a hypothetical unit molar fraction solution. The conversion between this state and the Ben-Naim definition at 25 °C is performed by

$$\begin{aligned}\Delta G^{*}_{\mathrm{solv}} &= \Delta G^{\mathrm{AL}}_{\mathrm{solv}} - RT\ln(d_{\mathrm{w}}\widetilde{R}T/M_{\mathrm{w}}) \\ &= \Delta G^{\mathrm{AL}}_{\mathrm{solv}} - 4.3\ \mathrm{kcal/mol}, \end{aligned} \quad (2)$$

where $\Delta G^{\mathrm{AL}}_{\mathrm{solv}}$ is the Gibbs free energy of hydration in the state reported by Abraham and Liszi, d_{w} the density of water under that temperature, and M_{w} the molar mass of water [37,41].

Combining the data for the aqueous free energy of solvation with the data for the free energy of transfer from water to the organic solvent, we obtained the free energies of solvation for our set of anions in AN and DMF. The experimental data collected by the described procedure are displayed in Table 1.

Gas phase geometry optimizations of the isolated anions were performed using the GAMESS package [42]. These calculations were performed at the Hartree-Fock RHF/6-31+G(d,p) level. The gas phase optimized geometries were used in the liquid phase calculations without any corrections. It has been noted that the use of gas phase geometries in the calculations for the solvation process does not introduce significant errors when compared to geometries optimized in solution [25].

In order to compute the solvation free energies, we adopted the PCM model, with the total solvation Gibbs free energy $\Delta G^{*}_{\mathrm{solv}}$ given by the sum of a cavitation energy term (ΔG_{cav}) which represents the work spent to build the solute cavity in the solvent, a solute/solvent van der Waals interaction term (ΔG_{vdW}), and a solute/solvent electrostatic polarization term (ΔG_{ele}) [26,43]. So we have,

$$\Delta G^{*}_{\mathrm{solv}} = \Delta G_{\mathrm{cav}} + \Delta G_{\mathrm{ele}} + \Delta G_{\mathrm{vdW}}. \quad (3)$$

In the following, we describe two methodologies for the calculation of $\Delta G^{*}_{\mathrm{solv}}$ in the anionic solutions. In our first theoretical approach, we consider only the electrostatic contribution to the solvation free energy of the set of anions. This term is known to dominate the solvation free energy of ions in polar solvents. The remaining contributions (cavitational and van der Waals) are small and in, most cases, somehow could be included in the definition of the scaling factor as it was discussed by Pliego and Riveros [29]. So in a first approach, we can consider,

$$\Delta G^{*}_{\mathrm{solv}} = \Delta G_{\mathrm{ele}}, \quad (4)$$

with

$$\Delta G_{\mathrm{cav}} + \Delta G_{\mathrm{vdW}} \approx 0. \quad (5)$$

As mentioned in the introduction, the choice of the solute's cavity size represents the central object of parameterization in the PCM. In our strategy to create the solute cavity, we started from the atomic radii of the atoms for the solute molecule and used the GEPOL-GAUSS-BONNET method [20,44]. For smoothing interatomic contact regions, we added smaller spheres with a minimum radius of 0.2 Å. This procedure removed the interspherical overlap.

Table 1
Experimental data for the Gibbs free energy of hydration $\Delta G^{*}_{\mathrm{hyd}}$, transfer from water to AN, $\Delta G^{*}_{\mathrm{trans}}$(AN), solvation in AN, $\Delta G^{*}_{\mathrm{solv}}$(AN), transfer from water to DMF, $\Delta G^{*}_{\mathrm{trans}}$(DMF), and solvation in DMF, $\Delta G^{*}_{\mathrm{solv}}$(DMF) for the set of anions (all values in kcal/mol)

Anion	$\Delta G^{*}_{\mathrm{hyd}}$	$\Delta G^{*}_{\mathrm{trans}}$(AN)	$\Delta G^{*}_{\mathrm{solv}}$(AN)	$\Delta G^{*}_{\mathrm{trans}}$(DMF)	$\Delta G^{*}_{\mathrm{solv}}$(DMF)
F^-	−105.0	+17.0	−88.0	+12.2	−92.8
Cl^-	−74.6	+10.1	−64.5	+11.5	−63.1
Br^-	−68.6	+7.5	−61.1	+8.7	−59.9
I^-	−59.9	+4.0	−55.9	+4.9	−55.0
I_3^-	−34.8	−3.6	−38.4	−6.4	−41.2
N_3^-	−70.7	+8.8	−61.9	+8.6	−62.1
CN^-	−67.6	+8.4	−59.2	+9.6	−58.0
SCN^-	−55.3	+3.4	−51.9	+4.4	−50.9
NO_3^-	−61.5	+5.0	−56.5	–	–
ClO_4^-	−51.3	+0.5	−50.8	+1.0	−50.3
$CH_3CO_2^-$	−77.3	+14.6	−62.7	+15.8	−61.5
Pic^-	−39.8	−1.0	−40.8	−1.7	−41.5

Table 2
Atomic radii (in Å) used in the definition of the solute cavities in the PCM model for the calculation of solvation free energies

Element	H	C	N	O	F	S	Cl	Br	I
Radius	1.20	1.70	1.60	1.50	1.35	1.85	1.81	1.95	2.15

The corresponding cavity has been increased by establishing a scaling factor multiplying the atomic radii. The optimized scaling factors have been determined by minimizing the average of absolute deviations between the calculated free energies of solvation and the experimental free solvation energies of the set of anions.

All the calculations in solution were performed using the GAMESS package at the same level of theory as the gas phase calculations. We have chosen the integral equation formalism IEF-PCM [20,21] and applied the charge renormalization by the method of Mennucci and Tomasi [45] in order to correct for charge density which escapes from the cavity, as implemented in the GAMESS package. For the optimized solute's cavities, the charge that escapes from the cavity is always less than 1% of the total electronic charge of the anion.

The atomic radii used in the definition of the cavities for the solutes are those stored in the GAMESS package. These atomic radii were taken from Emsley compilation [46] and modified by the Pisa group for the C, N and O atoms [20]. The used atomic radii are shown in Table 2.

The crucial step in the parameterization of PCM for using it in the computation of Gibbs free energies of solvation for a set of solutes in a given solvent is the determination of a suitable scaling factor for the atomic radii of the solute in the creation of the solutes' cavities. So this is our first task in the parameterization procedure which we refer to as Methodology I. We have searched for the best scaling factor by changing systematically its value between 1.00 and 2.00 and observing the mean absolute deviation between the set of results for the computed Gibbs free energy of solvation and the experimental data. The procedure has been applied until we found the minimum in the mean absolute error. The corresponding value for the scaling factor was chosen to be the scaling factor for the solutes' cavities in the solvent under consideration.

Having established a uniform scaling factor for the set of solutes in each solvent, we did not further modify the atomic radii in order to improve the theoretical results, but preferred to maintain the proportionality between the solute's cavities in the two solvents and previously reported studies. The solvent properties used here were taken from Riddick and Bunger [47]. Molecular radii for the solvents have been taken from Abraham and Liszi [37]. These empirical solvent data employed in the PCM are compiled in Table 3.

Table 3
Properties of the solvents AN and DMF at 298 K

	AN	DMF
Dielectric constant ϵ	35.94	36.71
Molecular radius/Å	2.137	2.647
Density/kg m^{-3}	776.49	943.87
Molar volume/cm^3 mol^{-1}	52.870	77.442

In the second part of this work, we performed the parameterization of the PCM model including explicitly the cavitation and van der Waals contributions to ΔG^*_{solv}. The cavities determined as described above have been established by minimizing theoretical free energies of solvation against experimental data. As a consequence, cavitational and van der Waals terms are empirically included in the scaling factors for the atomic radii and the obtained cavities can not furnish any independent information about ΔG_{cav} and ΔG_{el}. In order to establish cavities for the solutes that correspond to real liquid state configurations, we performed molecular dynamics (MD) simulations on a set of anions in AN and DMF solutions. MD simulations provide insight into the structure of the first solvation shell around the ions, and we have used this information to define suitable cavities for the anions in the continuum model. In particular, we adapted appropriate scaling factors for the atomic radii of the solutes from these structural data of the solutions in AN and DMF.

It is shown in the next section, where we report and discuss the results of MD simulations, that we can establish a connection between the solute–solvent radial distribution functions obtained in MD simulations and the surface of the cavity which defines the solute–solvent interface in the PCM model. The success of this methodology has been reported along the last years [16,27] and, for this reason, we also have chosen to apply it here. In order to investigate these structural properties, we have performed MD simulations on solutions of a single halide anion in liquid AN or DMF. The MD simulations were performed with the MDynaMix 4.3 software [48]. The force-field parameters for the halide anions (F^-, Cl^-, Br^- and I^-) were taken from the optimized parameters for liquid-phase simulation (OPLS) force field [49]. The acetonitrile solvent was modeled by the rigid body united-atom three-site model of Edwards et al. [50], and the united-atom OPLS description was used to model the DMF solvent molecules [51]. The potential parameters for the anions and the solvent molecules are summarized in Table 4. In the case of the DMF solvent molecules, the bond lengths and the bond angles were kept fixed, but the rotation about the C_O–N bonds was included in the simulations according to the original OPLS united-atom model for liquid amides. The Lorentz–Berthelot mixing rules were used to obtain the Lennard-Jones parameters for unlike atoms [7].

Molecular Dynamics simulations were carried out in the *NVT* ensemble for one of the halide ions (F^-, Cl^-, Br^- or I^-) and 255 solvent molecules (AN or DMF) initially

Table 4
Lennard-Jones parameters and partial charges in the intermolecular potential function models used in the molecular dynamics simulations of the solutions of halides (F^-, Cl^-, Br^- and I^-) in AN and DMF

Molecule	Atom type	σ/Å	ε/kJ mol^{-1}	q/e
AN	CH_3	3.60000	1.58810	0.269
	C	3.40000	0.41570	0.129
	N	3.30000	0.41570	−0.398
DMF	CH_3	3.80000	0.71120	0.285
	N	3.25000	0.71120	−0.570
	CH	3.80000	0.48120	0.500
	O	2.96000	0.87860	−0.500
F^-	F	2.73295	3.01248	−1.000
Cl^-	Cl	4.41724	0.49283	−1.000
Br^-	Br	4.62376	0.37656	−1.000
I^-	I	5.40000	0.29288	−1.000

arranged on a fcc lattice in a cubic box. The box dimensions were set according to the experimental densities (see Table 2) of the liquid solvents at simulation temperature (298 K). Periodic boundary conditions were used to mimic an infinite system and the minimum image convention was applied. Long range electrostatic interactions were taken into account by the Ewald summation method [52]. We applied a cutoff radius of 14 Å and 16 Å to the AN and DMF simulations, respectively. The equations of motion were integrated using the Tuckerman–Berne algorithm [53] with the long time step of 2 fs and the short time step of 0.2 fs. The temperature was maintained by the Nosé-Hoover thermostat with a coupling constant of 30 fs [54]. The bond lengths and bond angles were kept rigid by employing the SHAKE algorithm [55]. Results of the MD simulations were obtained from production runs of 100 ps that were preceded by a stabilization period of 200 ps. The thermodynamic averages and atom–atom pair distribution functions were computed from configurations saved in intervals of 10 time steps.

The radial distribution functions (RDFs) for X–S atom pairs, where X is one of the four halide anions and S is an appropriate solvent site, were computed from the MD simulations of the anion solutions in AN and DMF. The radial distance corresponding to the maximum in the first peak of the RDFs was utilized to localize the average position of the S sites within the first solvation shell around the anions. This information about the solvent structure around the solutes was used to define the scaling factor applied to the cavity creation for the solutes in the PCM model. Once the suitable cavities and the respective scaling factors for the atoms of the anion solutes were established, we performed the calculation of the electrostatic and cavitation terms in the total free energy of solvation for the set of anions.

In order to study in more detail the structure of the first solvation shell of the anions in AN and DMF solutions, we have also carried out *ab initio* calculations of ion–solvent complexes. In these simulations, the anionic solute is complexed by a few solvent molecules and the system (solute + solvent molecules) is treated quantum mechanically.

According to the information obtained from the MD simulations, the AN solvent molecules arrange around the negatively charged halide solutes with their methyl groups pointing to the anionic solute. In the case of the DMF solutions, it is the methyl group in the position opposite to the oxygen atom that points to the anionic solute. With this information coming from the MD simulations, we were able to build the initial configuration for the ion–solvent complexes. In addition, the MD simulations indicate that the number of AN solvent molecules in the first solvation shell around the halide solutes is about six. So we have built complexes containing one halide atom in the center and six AN molecules around it. For the DMF complexes, we have used one halide atom and only three DMF solvent molecules due to restrictions in our limited computational facilities for calculating a system containing six DMF solvent molecules and the solute on the *ab initio* level. The molecular geometries of these complexes were optimized in the gas phase without any constraints on atomic positions or particular symmetries. The *ab initio* computations were carried out at the RHF/6-31+G(d,p) level of theory and the minimum energy configuration of the complexes were checked by normal mode analysis demonstrating the absence of imaginary frequencies. From the final structures of the complexes we elucidated distances between the central halide atoms (F, Cl or Br) and the methylic hydrogen atoms of the solvent as well as the angles X–H–C (X=F, Cl or Br). These results are reported in the next section.

In this second proposal for the computation of the Gibbs free energy of solvation for the anions in AN and DMF, referred to as Methodology II, ΔG^*_{solv} is computed explicitly from the three contributions indicated by Eq. (3). The electrostatic component (ΔG_{ele}) was computed using the IEF-PCM method with same procedure described in the Methodology I, but now from scaling factors established from structural data obtained via MD simulations. The free energy of cavitation (ΔG_{cav}) is a measure for the work necessary to insert the solute with its cavity into the solvent. This term was computed by the Claverie–Pierotti formalism making use of scaled particle theory and molecular cavities as described in Ref. [43,56,57]. The physical parameters of the solvent required in the calculation of the cavitation energy are the solvent radius, the molecular weight and the density (see Table 3). The van der Waals repulsion–dispersion energy contribution was computed using a linear relationship between this term and the solvent accessible surface area of the N atoms of the solute,

$$\Delta G_{vdW} = \sum_{i=1}^{N} \xi_i A_i, \tag{6}$$

where A_i is the solvent accessible surface area of the atom i and ξ_i defines the van der Waals parameter for the atom i relating its surface area to the van der Waals energy contribution [26,43]. The atomic van der Waals parameters ξ_i were optimized by a multiple linear regression procedure

[58]. In this procedure, we minimized the difference between the experimental solvation free energies and the sum of computed electrostatic and cavitation free energy contributions,

$$\Delta G_{\mathrm{vdW}}(A_i;\xi_i) = \text{minimum}\{\Delta G_{\mathrm{solv}}(\exp) - \Delta G_{\mathrm{ele}} - \Delta G_{\mathrm{cav}}\}. \quad (7)$$

Thus, one of the basic steps in the second methodology of parameterization is represented by the optimization of the van der Waals parameters. The van der Waals energy is determined as an empirical term, which is included in order to obtain the best correlation between the calculated solvation free energies and the experimental data. More details on these procedures are given in the next section where we present the corresponding results.

3. Results and discussion

We begin with the parameterization procedure characterized above as Methodology I, in which we assume the validation of Eq. (4) considering the solvation free energy as purely electrostatic. Using the gas phase geometries for the anions listed in Table 1 and representing the atoms by spheres possessing the radii from Table 2 multiplied by the scaling factor, the free energies of solvation computed from the PCM was compared with the corresponding experimental value. The obtained mean absolute deviations between calculated and experimental $\Delta G^*_{\mathrm{solv}}$ for the complete set of anions are illustrated in Figs. 1 and 2 as a function of the scaling factor for the AN and DMF solvents, respectively. For both solvents, we observe a minimum in the mean absolute deviation corresponding to a scaling factor of 1.36 for the solute cavities in AN and 1.39 in DMF solutions.

Having established the scaling factors for the cavities in the two solvents, we examine the overall performance of Methodology I. Therefore, we computed the free energy of solvation for each anion employing the optimized scaling parameters (AN: 1.36 and DMF: 1.39). The comparison of the computed $\Delta G^*_{\mathrm{solv}}$ with the experimental results is presented in Table 5 for the set of anions solvated in AN and in Table 6 for solvation in DMF. The correlations between theoretical results and experimental solvation free energies in AN and DMF are displayed in Figs. 3 and 4, respectively.

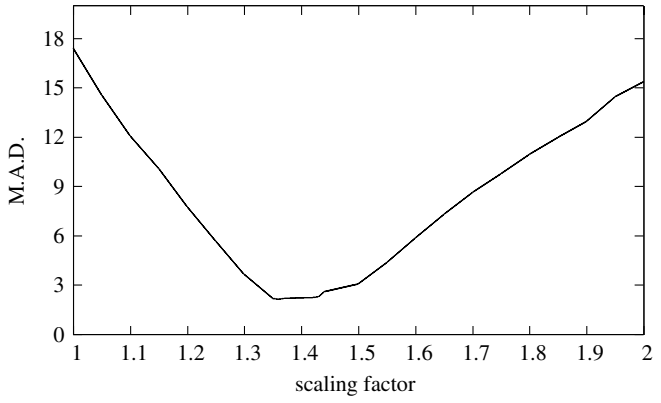

Fig. 1. Mean absolute deviation, MAD (in kcal/mol), against the scaling factor adopted to the atomic radii from Table 2 in the cavity creation for the solvent AN.

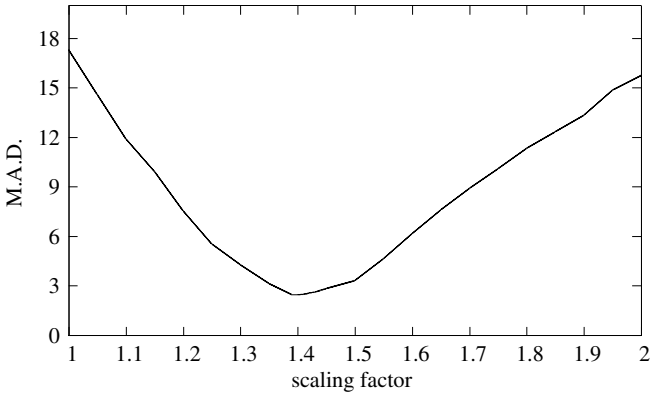

Fig. 2. Same as Fig. 1, but for the DMF solvent.

In the case of the AN solvent, we observe in Fig. 3 a nice distribution of at least seven of the twelve points around the straight line that corresponds to perfect agreement between the two data sets. For the remaining five solutes, the computed free energy of solvation is slightly more negative than the experimental value. Thus, the overall performance of the parameterization for the PCM in AN produces a very good correlation between computed and experimental solvation free energies by the procedures of Methodology I, with the optimized scaling factor of 1.36.

A similar conclusion is also valid for the anionic DMF solutions in Fig. 4 with the computed free energies of solvation obtained from the optimized scaling factor of 1.39. For at least eight of the eleven anions in the set, the computed results present excellent correlation with the experimental data.

Table 5
Free energies of solvation (in kcal/mol) calculated, $\Delta G^*_{\mathrm{solv}}$(calc), and experimental, $\Delta G^*_{\mathrm{solv}}$(exp), for the anions in AN in the electrostatic approach with the optimized value of 1.36 for the scaling factor of radii

Anion	$\Delta G^*_{\mathrm{solv}}$(calc)	$\Delta G^*_{\mathrm{solv}}$(exp)	Error
F^-	−86.8	−88.0	+1.2
Cl^-	−64.6	−64.5	−0.1
Br^-	−59.9	−61.1	+1.2
I^-	−55.2	−55.9	+0.7
I_3^-	−38.3	−38.4	+0.1
N_3^-	−61.7	−61.9	+0.2
CN^-	−63.6	−59.2	−4.4
SCN^-	−57.4	−51.9	−5.5
NO_3^-	−60.2	−56.5	−3.7
ClO_4^-	−53.9	−50.8	−3.1
$CH_3CO_2^-$	−64.4	−62.7	−1.6
Pic^-	−44.8	−40.8	−4.0
Mean absolute error			2.2
Mean error			−1.6
SD			2.4

Table 6
Calculated ΔG^*_{solv}(calc) and experimental ΔG^*_{solv}(exp) free energies of solvation (in kcal/mol) for the anions in DMF obtained using the optimized scaling factor of 1.39 in the electrostatic approach

Anion	ΔG^*_{solv}(calc)	ΔG^*_{solv}(exp)	Error
F^-	−85.1	−92.8	+7.7
Cl^-	−63.4	−63.1	−0.3
Br^-	−58.8	−59.9	+1.1
I^-	−54.2	−55.0	+0.8
I_3^-	−41.2	−41.2	0.0
N_3^-	−61.1	−62.1	+1.0
CN^-	−62.5	−58.0	−4.5
SCN^-	−55.4	−50.9	−4.5
ClO_4^-	−53.6	−50.3	−2.9
$CH_3CO_2^-$	−63.3	−61.5	−1.8
Pic^-	−43.7	−41.5	−2.2
Mean absolute error			2.5
Mean error			−0.5
SD			3.4

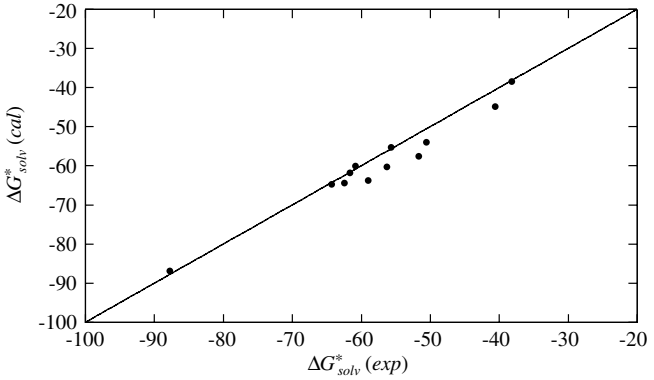

Fig. 3. Comparison between calculated ΔG^*_{solv}(calc) and experimental ΔG^*_{solv}(exp) free energies of solvation (in kcal/mol) for the anions in AN, using the pure electrostatic energy approach. The line indicates perfect correlation.

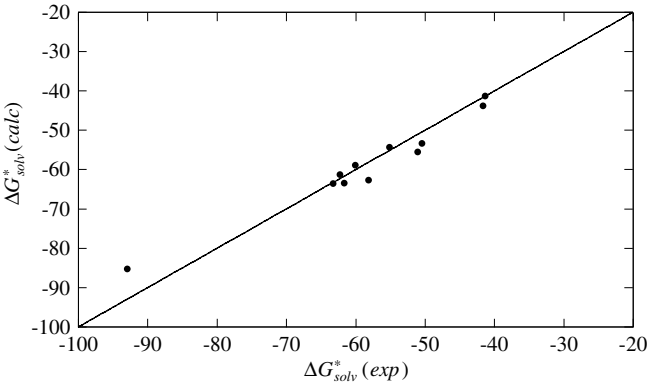

Fig. 4. Same as Fig. 3, but for the DMF solutions.

The statistical analysis of the differences between computed and experimental free energies of solvation in AN (Table 5) produces a mean absolute deviation, or mean unsigned error, of 2.2 kcal/mol. The mean signed error is −1.6 kcal/mol with a standard deviation of 2.4 kcal/mol. For the DMF solutions, the data from Table 6 furnish a mean absolute deviation of 2.5 kcal/mol, a mean signed error of −0.5 kcal/mol and a standard deviation of 3.4 kcal/mol.

We analyze and discuss some of the most important observations in the results displayed by Tables 5 and 6. Solvation of the F^- anion in AN produced a value for the solvation free energy that is 1.2 kcal/mol higher than the experimental value. If we take into account that the uncertainty associated with the experimental value in the solvation energy for this anion is approximately ±1.6 kcal/mol [31,59], we consider our theoretical result in excellent agreement with experiment. In DMF, we obtained a value exhibiting a positive deviation of 7.7 kcal/mol. This is the worst deviation of all the anions considered by Methodology I. At first sight, it seems that the pure electrostatic energy approach from Eq. (4) fails in modeling the solvation of F^- anion in DMF. And it is likely in this case that the steric and van der Waals terms of the Gibbs free energy of solvation also play an important role in the solvation of this anion in DMF and do not cancel as indicated by Eq. (5).

In the cases of the other halide anions (Cl^-, Br^-, and I^-), the deviations between theoretical and experimental solvation free energies are very small within the range of experimental uncertainties. Thus, Methodology I represents a suitable approach for computing the Gibbs free energies of solvation of these anions in AN and DMF.

Considering the anions CN^-, SCN^-, NO_3^-, ClO_4^- and Pic^-, the theoretical approach to ΔG^*_{solv} produced negative deviations from the experimental data. For these anions, Methodology I apparently is affected by a systematic error related to the approximations involved in Eq. (4). The worst case in AN is the anion SCN^- with an error of −5.5 kcal/mol. We also observe an error of −4.5 kcal/mol in the energy of solvation for the SCN^- anion in DMF and −2.9 kcal/mol for the ClO_4^- anion.

Especially the case of the ClO_4^- anion deserves a more detailed discussion. For this particular anion, there is a controversy with respect to the experimental free energy of solvation. In this present study, we have adopted the experimental free energies of solvation for the ClO_4^- anion in AN (−50.8 kcal/mol) and DMF solutions (−50.3 kcal/mol) from Abraham and Liszi [37]. Alternatively, we could have used the hydration free energy and transfer energies published in the different Marcus compilations [34,31,60]. In Ref. [60], the experimental solvation energy for the ClO_4^- anion in water is −102.8 kcal/mol. Using this value combined with the data of the free energies of transfer between water and AN or DMF, we obtain −102.2 kcal/mol for the free energy of solvation in AN and −101.8 kcal/mol for the solvation energy in DMF. Both values are approximate 50 kcal/mol more negative than the experimental data presented in Ref. [37]. A slightly more recent publication [34] presents −49.0 kcal/mol as the experimental hydration free energy for the ClO_4^- anion. Combining this experimental value with the free energy of transfer data, we obtain the free energy of solvation in AN

as −48.5 kcal/mol and as −48.0 kcal/mol for solvation in DMF. If we compare the experimental data obtained from these sources with our results, we notice that the theoretical results are closer to the data provided in Ref. [37]. Thus, our theoretical results may suggest that the experimental hydration free energy for ClO_4^- probably is not correct in Ref. [60] and the solvation free energies provided by Abraham and Liszi [37] should be adopted for this anion in the solvents AN and DMF.

In the following, we further discuss apparent problems with experimental data of thermodynamic properties for ion solvation. However, it is not our purpose here to describe and discuss the experimental procedures involved in the determination of thermodynamic functions for ion solvation. These details, including additional extra-thermodynamic assumptions involved in the experimental strategies to single ion solvation free energies, have already been addressed in various publications [5,31,32,61,62]. These references present the principles for measuring and obtaining the infinite dilution single ion thermodynamic functions in the processes of transferring ions from one solvent phase to another. We want to stress that the experimental estimation of the Gibbs free energy of transfer for ions between two solvents might involve some details that are not considered in the theoretical description, but might be related to the deviations between experimental and computed free energies of solvation, especially for the ClO_4^-, SCN^- and picrate anions. According to Marcus, there are some complications in the experimental determination of the thermodynamic quantities involved in the ion transfer. One of these complications is the possibility of ion pairing in solvents with moderate or low relative permitivities. Another complication is the coextraction of the reference solvent in the process of transferring some anions from one solvent to the other [63]. Especially this second point represents a major problem in the determination of thermodynamic functions for ion transfer between aqueous and organic phases [36,64].

Studies on ion–solvent interactions in AN solutions of lithium and sodium perchlorate indicate the formation of ion pairs over a wide range of concentrations [65]. Thus, the ion-ion interactions complicate the separation of the individual ionic contributions to thermodynamic transfer functions for the electrolytes. Similar studies have been undertaken in DMF solutions of lithium and sodium perchlorate also exhibiting evidences for the existence of both, solvent shared and contact solvated ion pairs [66]. Studies on the structure of $NaClO_4$ solutions in DMF also furnished experimental evidences for the formation of ion pairs shared by solvent molecules. These complexes might be responsible for significant deviations of the experimental free energy of transfer, solvation free energies, or other thermodynamic properties from the single ion limit. Depending on the particular structures of the complexes, these deviations point toward positive or negative values [67].

The problem of coextraction of solvent molecules in the ion transfer processes, especially in the transfer from water to organic solvents, has also been observed in experimental studies. Osakai et al. [68] found that some ions, such as SCN^-, ClO_4^- and picrate, are transferred from water to organic solvents as hydrated ions. As an additional effect, the symmetry break in the anion structure due to coordinated water molecules might change the charge distribution of the anion and, consequently, affect the solvation energy for the anion in the transfer process. Thus, there are problems in the experimental estimate of thermodynamic quantities for these ions in solution. The theoretical concept is based on the postulate that a single ion is transferred without any solvent molecules from the original solvation shell. The mentioned experimental difficulties require a new approach to the treatment of the Gibbs free energy of ion transfer taking into account the partial hydration of these anions when being transferred to organic solvents [68].

Of course, in our continuum formulation of anion solvation, we ignored the problems that are not included in the basic assumptions for the treatment of experimental results and the calculation of the thermodynamic quantities of transfer. These quantities are always referred to single ion contributions without the transport of solvent between two separated phases [63]. Thus, it appears that the differences between theoretical and experimental Gibbs free energies of solvation for the SCN^-, ClO_4^- and picrate anions may be partially related to experimental problems. The experimental free energy of solvation for these ions used as a reference in this work is based on transfer data and possibly affected by errors. Thus, the theoretical studies carried out in the present work on solvation in AN and DMF may contribute to solve problems for the correct determination of Gibbs free energies of transfer between water and organic solvents as well as in the accurate determination of Gibbs free energies of solvation for anions in organic solvents.

The relatively large negative deviation in the computed free energies of solvation for the picrate anion (−4.0 kcal/mol in AN and −2.2 kcal/mol in DMF) indicates that our Methodology I possibly fails in describing correctly the solvation process as purely electrostatic. The picrate anion is larger than the other ions studied here and one might expect for larger ions that steric terms represent an important contribution to the total solvation energy [69–71]. Results obtained from the inclusion of the steric terms by our Methodology II (see below) support this possibility.

Most of the anions studied by Methodology I demonstrate a good agreement between calculated and experimental Gibbs free energies of solvation, with errors smaller than the range of the experimental uncertainty of ±6.0 kcal/mol in this property obtained from ion transfer data [35,63]. Considering the entire set of anions, we have obtained results with a mean absolute deviation of 2.2 kcal/mol in the solvation free energies in AN and a mean absolute deviation of 2.5 kcal/mol for the free energies in DMF. These errors are comparable with the errors found in parameterizations of continuum models for the study of ionic solvation in water and DMSO [27,29,72,28].

The scaling factors for the atomic radii obtained in our parameterization for AN and DMF solutions, 1.36 and 1.39, respectively, are very similar to the scaling factor 1.35 reported for the parameterization of DMSO [29]. Similar scaling factors are expected for all of these solvents representing polar aprotic solvents. The small differences in the scaling factors reflect the different global solvent parameters (dielectric constant, size of the solvent molecules). The scaling factors for these polar aprotic solvents are larger than the scaling factor of 1.15 obtained for water [27] indicating that the first shell solvent molecules are closer to the solvated anions in water than in polar aprotic solvents. Thus, these simple parameterization procedures are capable to verify the experimental observation that anions are better solvated by water than by polar aprotic solvents [4].

Within the context of the purely electrostatic continuum methodology that we are applying to the computation of the Gibbs free energy of solvation for anions, it is also interesting to perform some comparisons with the Born Model for ion solvation. As in our Methodology I, the Born Model for ion solvation also considers that the Gibbs free energy of solvation is given by the electrostatic interactions of the ion with the continuum. In the model proposed by Born, the change in the Gibbs free energy that occurs when an ion is transferred from the gas phase into the solvent, depends on the charge of the ion Z_i, the ion radius r_i, and the dielectric constant ϵ of the medium. In terms of these variables, the free energy of solvation is expressed by,

$$\Delta G_{\text{solv}} = -\left(\frac{\epsilon - 1}{\epsilon}\right)\frac{N_{\text{A}}(Z_i e_0)^2}{2r_i}, \tag{8}$$

where N_{A} represents Avogadro's number and e_0 the elementary charge [73]. It has been stated that the solvation free energy of ions can be represented by a pure electrostatic Born term, if an effective Born radius is chosen for the ion [73–75]. In order to verify this statement, we have performed the calculation of the effective Born radii that yields the experimental free energies in AN and DMF from Eq. (8) for some anions using the solvent properties from Table 3. We compare the effective Born radii in Table 7 with effective radii of the cavities (for the spherical halide anions) in the PCM approach. We can notice that the effective Born radius and the solute's cavity radius are very close to each other. However, this relationship holds only for the spherical halide anions. For non-spherical ions like the N_3^- anion or the picrate anion, it would be very difficult to give a consistent definition of an effective Born radius. For the N_3^- anion, the calculated effective Born radius in AN is 2.53 Å, and for the Pic^- anion this radius is 3.78 Å. Similar values are found for DMF solutions. These results show that the effective Born radii become physically unrealistic for non-spherical ions because these effective Born radii are much smaller than the gas phase radii as estimated from *ab initio* calculations of these anions. Thus, these solutes are examples that do not fit into the Born model. In these cases, the PCM model is more efficient and realistic treating solutes of arbitrary shape and providing valuable information in addition to the thermodynamic properties of solvation, such as changes in the wave function and charge distribution of the solute in solution. On the other hand, these results also help to verify the consistency of the PCM model when the cavity size is comparable to that of Born model. We observe similar values for the effective radii of the cavities based in the classical electrostatic Born model and the PCM which is based in wave function derived charges on the cavity surface.

Table 7
Solute radius in comparison with effective Born radius R_{Born} and effective PCM radius R_{PCM} for some anions in AN and DMF

Anion	Radius	R_{Born}(AN)	R_{PCM}(AN)	R_{Born}(DMF)	R_{PCM}(DMF)
F^-	1.35	1.80	1.81	1.71	1.70
Cl^-	1.81	2.43	2.47	2.48	2.53
Br^-	1.95	2.56	2.59	2.61	2.67
I^-	2.15	2.79	2.88	2.84	2.94
N_3^-	–	2.53	–	2.52	–
Pic^-	–	3.78	–	3.72	–

All radii in Å.

In the following, we report our results for the solvation of anions in AN and DMF solvents from the procedures that we called Methodology II. In this second proposal, we performed the complete parameterization of the three contributions ΔG_{cav}, ΔG_{ele}, and ΔG_{vdW} from Eq. (3) for the IEF-PCM model aiming at the application to anionic solutions in AN and DMF.

In this second methodology, the scaling factor for the atomic radii is established from MD simulations of the anionic solutions and does not stem from any parameterization procedures involving the free energy of solvation. Thus, in our Methodology II, both, the electrostatic contribution ΔG_{ele} and the cavitational term ΔG_{cav} from Eq. (3), become independent of experimental data. Therefore, the objects for the parameterization are the van der Waals atomic hardness ξ_i, or van der Waals coefficients that establish a linear relationship between the solvent exposed surface area of the atoms in the solutes and their contribution to the van der Waals energy as defined by Eq. (6).

We begin the discussion of the procedures for Methodology II with the results of the MD simulations of the anionic solutions. In general, data obtained from MD simulations depend on the applied physical model. In our case, the results we report here for the properties of ions in solution are sensitive to the parameters used to describe the solvent molecules and the ions. The solvent structure around an ion may vary depending on the force-field parameters chosen for the simulations. As a consequence, the free energy of solvation calculated by a continuum model that makes use of simulated structural data is also dependent on the parameters and procedures adopted to the MD simulations of the anionic solutions in AN and DMF.

From the MD simulations of halide anions in AN and DMF, we computed the X–S radial distribution functions, with X being the halide anion (F^-, Cl^-, Br^- and I^-) and S

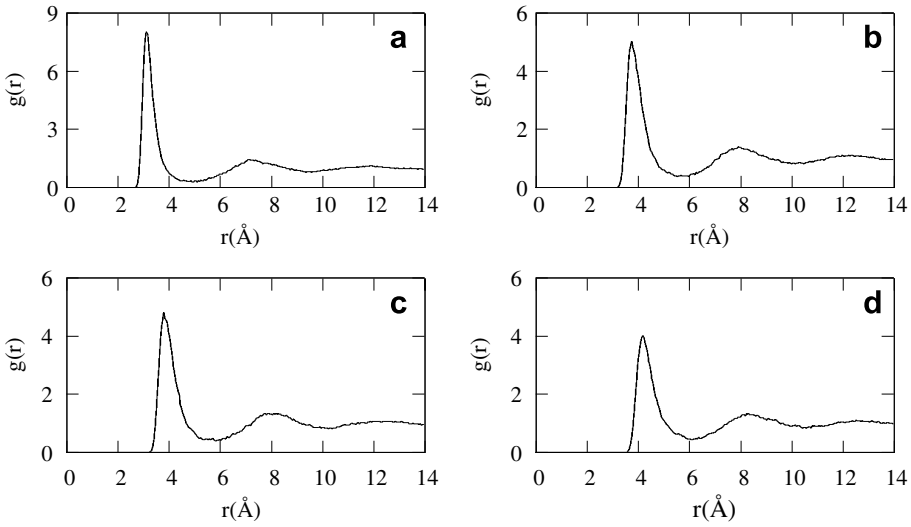

Fig. 5. Radial distribution functions $g(r)$ for anionic halide solutions in AN at infinite dilution obtained from MD simulations: (a) RDF for F^-–CH_3 pairs; (b) RDF for Cl^-–CH_3 pairs; (c) RDF for Br^-–CH_3 pairs; (d) RDF for I^-–CH_3 pairs.

one of the solvent sites. In the PCM approach, the surface of the solute's cavity represents the boundary between solute and dielectric continuum. Thus, in order to define this boundary, we are interested only in the solvent site S that corresponds to shortest X–S distances. A first analysis of the RDFs demonstrated that shortest distances X–S are due to the X–CH_3 pairs. In the case of the DMF solutions, the two methyl groups produce different RDFs, with the shorter X–CH_3 distances corresponding to the CH_3 group located in trans position to the carbonyl group in the DMF molecule. We selected these RDFs describing shortest X–S pairs for further analysis.

In Fig. 5, we have displayed the X–CH_3 RDFs for the halides anions in AN solutions. For all the four anions studied in AN, these RDFs present an intense sharp first peak, a second broader peak with less amplitude, followed by more diffuse peaks. The average distance of the first shell methyl groups around the halide anions is defined by the maximum position of the first peak. From the RDFs in Fig. 5 we have determined the average X–CH_3 distances in AN given in Table 8. In order to correct for the united atom approach employed in the simulations, we have also calculated the average distances of the methylic hydrogens around the anions by subtracting the equilibrium C–H bond length in the CH_3 group (1.107 Å [76]) from average X–CH_3 distances. We illustrate this procedure for the F^- solutions. The maximum of the first peak in the RDF F–CH_3 corresponds to $r_{max} = 3.103$ Å. Subtracting 1.107 Å, we established the average distance $d_{F^-\text{–}H} = 1.996$ between the anion and a hydrogen atom of the solvent molecule. The computed average X–H distances, also included in Table 8, represent distances for closest atom pairs utilized to define the solute's cavity in real liquid configurations. The numerical values for the distances from Table 8 reproduce perfectly the physical picture that larger first shell distances appear in solutions of the larger solutes.

Table 8
Position of the maximum in the first peak r_{max} for the X–CH_3 RDFs in the solvent AN, distance between solute and methylic hydrogens $d_{X^-\text{–}H}$, and scaling factors computed from these data

Anion	r_{max}	$d_{X^-\text{–}H}$	Factor
F^-	3.103	1.996	1.48
Cl^-	3.757	2.650	1.46
Br^-	3.803	2.696	1.38
I^-	4.177	3.070	1.43
Average factor			1.44

r_{max} and $d_{X^-\text{–}H}$ in Å.

We have chosen to simulate only the solutions of the halide anions. In these cases, the solutes possess spherical symmetry which facilitates the task to establish a connection between distances obtained from RDFs and suitable positions of the solute's cavity in the PCM formalism. Comparing the distances X–H with the atomic radii r_i from Table 2, it is possible to define the ratio $d_{X^-\text{–}H}/r_i$ as the scaling factor for the atomic radii of the solutes. In the case of the F^- solutions, the F–H distance has been determined as 1.996 Å. Thus, dividing by the atomic radius 1.35 Å for the fluorine, we obtain the corresponding scaling factor of 1.48. The other halides have been treated by the same procedure. The calculated scaling factors (see Table 8) are 1.46, 1.38, and 1.43 for the Cl^-, Br^-, and I^-, respectively, for the halide anions in AN.

The similarity of these scaling factors encouraged us to compute an average scaling factor of 1.44 for the solvent AN and to define this average as a proportionality constant between the atomic radii and the boundary separating solute and solvent in real liquid configurations. Consequently, we applied this averaged scaling factor to all the atoms listed in Table 2 permitting the use of the PCM model for AN solutions of the all the anions studied in the present

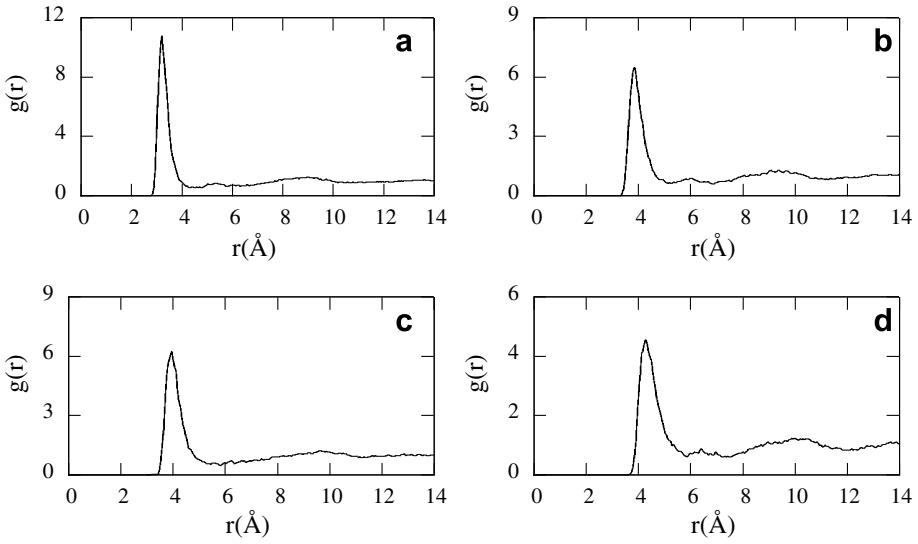

Fig. 6. Same as Fig. 5, but for the DMF solutions: (a) RDF for F^-–CH_3 pairs; (b) RDF for Cl^-–CH_3 pairs; (c) RDF for Br^-–CH_3 pairs; (d) RDF for I^-–CH_3 pairs.

work. In doing so, we suppose that the solvent molecules are arranged at the same preferential orientation with respect to all the solutes.

The solvent DMF has been treated by the same procedure. From the MD simulations, the methyl group in trans position to the carbonyl oxygen was identified as the closest solvent site to the halide anions. The corresponding RDFs are shown in Fig. 6. All these functions exhibit a sharp first peak with maximum positions listed in Table 9. Subtracting the C–H equilibrium bond length in the methyl group of the DMF molecule (1.107 Å [77]) from these maximum positions, we correct for the united atom approach in the simulations and obtain the average X–H distances from Table 9 for the nearest neighbor DMF molecules around the halide anions. The comparison with the atomic radii from Table 2 furnishes the scaling factors listed in the last column of Table 9. Again, we obtained very similar scaling factors for the four halide ions. Averaging yields an effective scaling factor of 1.52 for DMF solutions. As in the case of the solvent AN, this scaling factor has been employed in the PCM calculations of all the anions.

If we compare the scaling factors of 1.44 for anions dissolved in AN and 1.52 for the anionic solutions in DMF, we find, as in the purely electrostatic approach described by Methodology I, that the cavities for the anions are slightly larger in DMF.

Table 9
Same as Table 8, but for the DMF solutions

Anion	r_{max}	$d_{X^-–H}$	Factor
F^-	3.227	2.132	1.58
Cl^-	3.867	2.772	1.53
Br^-	3.973	2.878	1.47
I^-	4.293	3.198	1.49
Average factor			1.52

As mentioned above, data extracted from MD simulations involve always a force field dependence. In order to verify this effect on the scaling factors established from MD simulations, we also carried out *ab initio* studies of the complexes formed by halide anions (F^-, Cl^- and Br^-) and the solvent molecules of AN and DMF. We studied the molecular geometry of the complexes containing one halide atom and six molecules of the solvent AN. For DMF, we studied the complexes containing three solvent molecules.

Principal geometrical parameters obtained from these calculations are demonstrated in Table 10 and representative structures are shown in Fig. 7. Again, we have compared distances between the halide anions and the methylic hydrogens with the atomic radii of the halide anions defining the scaling factors. The numerical values for these factors are also given in Table 10. Averages for these scaling factors are 1.47 for complexes with AN and 1.55 for the DMF complexes.

If we observe the distances and angles of the hydrogen bonds in the complexes with AN, we conclude that the

Table 10
Some gas phase geometrical properties for the anion–solvent complexes

Complex	d(X–H)	d(X–C)	∠(X–H–C)	Factor
$[F(CH_3CN)_6]^-$	2.042	3.130	179.72	1.51
$[Cl(CH_3CN)_6]^-$	2.700	3.767	168.30	1.49
$[Br(CH_3CN)_6]^-$	2.759	3.840	176.80	1.42
$[F(DMF)_3]^-$	2.083	3.112	157.61	1.54
$[Cl(DMF)_3]^-$	2.825	3.845	158.20	1.56
$[Br(DMF)_3]^-$	2.997	3.801	140.49	1.54

d(X–H) is the average bond distance halide–solvent methylic hydrogen, d(X–C) the halide–solvent carbon average distance, ∠(X–H–C) the average angle between halide atom, hydrogen, and methyl carbon of the solvent molecules, as well as computed scaling factors. Distances in Å, angles in degrees.

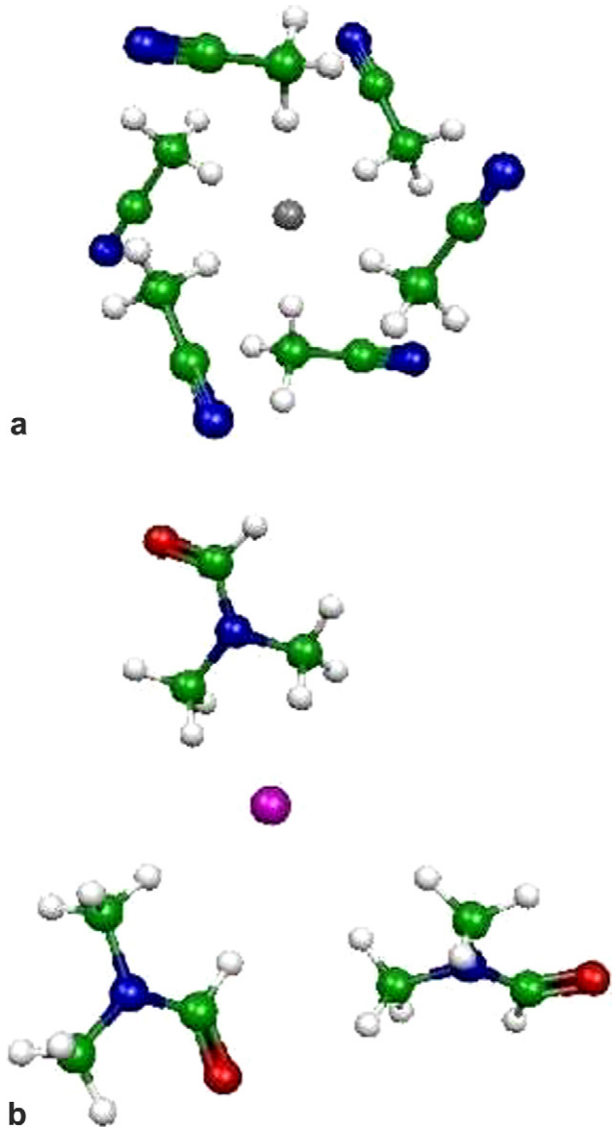

Fig. 7. Complexes of anion solutes with solvent molecules in gas phase: (a) $[F(CH_3CN)_6]^-$ and (b) $[Cl(DMF)_3]^-$.

protons of the solvent in the first solvation shell around the F^-, Cl^- and Br^- anions are located at an average distance that is approximately 1.47 times the atomic radii of these solutes. This value is very close to the value of 1.44 obtained from the MD simulations on AN solutions. Thus, the results extracted from the supermolecule calculation for the anion solutions validate our approach to establish the scaling factor utilizing structural data from MD simulations.

Similar conclusions can be drawn from the results obtained for the complexes containing the solvent DMF. The average distance of the solvent hydrogen atoms in the first solvation shell around the anions is nearly 1.55 times the atomic radii of the solutes which confirms nicely the numerical value of 1.52 for the scaling factor obtained from the MD simulations.

We mention that it is not our objective to study here thoroughly the structural aspects of the solvation of anions, but only to find a physical sense and interpretation for the parameters defining the cavities for the anions in the PCM computations of solvation in AN and DMF. For more detailed studies of the structures of the complexes of halides with solvents the reader is invited to consult the references [78–82].

Using the established scaling factors for atomic radii in the solute cavities (AN: 1.44, DMF: 1.52), we computed the electrostatic and cavitation components of the solvation free energy for the anions in the respective solvents as described in the previous section. Afterwards, we carried out the optimization of the van der Waals coefficients for all the atoms present in our set of solutes. The procedures have been outlined by Eqs. (6) and (7). Utilizing the multiple linear regression procedure in the minimization of the difference between the experimental solvation free energy and the sum of electrostatic and cavitational contributions for the complete set of solutes, we obtained the van der Waals parameters summarized in Table 11. Finally, the optimized van der Waals coefficients were employed in the computation of the van der Waals free energy contribution to the solvation free energy for the set of anions in AN and DMF. Therefore, the process of parameterization of the IEF-PCM model is complete for the study of the solvation thermodynamics of anions in these two solvents, including the electrostatic and the steric contributions to the solvation free energy of the set of anions under study.

Adding the three contributions, electrostatic (ΔG_{ele}), cavitation (ΔG_{cav}) and van der Waals (ΔG_{vdW}), we computed the Gibbs free energy of solvation (ΔG_{solv}) for the anions in the respective solvents. In Table 12, we present these data for the anion solutions in AN, and in Table 13, results for the solvent DMF are shown. The correlation between experimental and computed Gibbs free energies of solvation for Methodology II is displayed in Figs. 8 and 9 for the solvents AN and DMF, respectively.

The mean absolute deviation between computed and experimental Gibbs free energies of solvation in AN is 0.7 kcal/mol. The average error, including the sign of individual deviations is 0.2 kcal/mol and the standard deviation of the results is 1.5 kcal/mol. The statistical analysis for the results in DMF produces a mean signed error of 0.2 kcal/mol, a mean absolute deviation of 0.5 kcal/mol,

Table 11
Atomic van der Waals hardness parameters ξ_i (in kcal Å^2/mol) optimized for the computation of the van der Waals free energy contribution of the solvation of anions in AN and DMF

Atom	ξ_i (AN)	ξ_i (DMF)
H	−0.3083	−0.3126
C	−0.0820	−0.0828
N	−0.1732	−0.1804
O	−0.1253	−0.1031
F	−0.4026	−0.7641
S	−0.0852	−0.1087
Cl	−0.2055	−0.2223
Br	−0.2164	−0.2254
I	−0.1059	−0.1300

Table 12
Computed electrostatic, ΔG_{ele}, cavitational, ΔG_{cav}, and van der Waals, ΔG_{vdW}, contributions to the solvation free energies, ΔG^*_{solv}(calc) for anions in AN

Anion	ΔG_{ele}	ΔG_{cav}	ΔG_{vdW}	ΔG^*_{solv} (calc)	ΔG^*_{solv} (exp)	Error
F^-	−82.3	3.5	−9.2	−88.0	−88.0	0.0
Cl^-	−61.4	5.5	−8.5	−64.4	−64.5	+0.1
Br^-	−56.9	6.1	−10.3	−61.1	−61.1	0.0
I^-	−52.4	7.2	−6.2	−51.4	−55.9	+4.5
I_3^-	−42.7	17.2	−14.7	−40.2	−38.4	−1.8
N_3^-	−60.0	7.8	−9.6	−61.8	−61.9	+0.1
CN^-	−60.5	6.4	−5.7	−59.8	−59.2	−0.6
SCN^-	−53.6	9.3	−7.6	−51.9	−51.9	0.0
NO_3^-	−57.4	9.0	−8.1	−56.5	−56.5	0.0
ClO_4^-	−52.3	11.3	−10.5	−51.5	−50.8	−0.7
$CH_3CO_2^-$	−61.2	11.8	−13.5	−62.9	−62.7	−0.2
Pic^-	−42.8	27.6	−25.2	−40.4	−40.8	+0.4
Mean absolute error						0.7
Mean error						0.2
SD						1.5

Table 13
The same as in Table 12, but for the DMF solutions

Anion	ΔG_{ele}	ΔG_{cav}	ΔG_{vdW}	ΔG^*_{solv} (calc)	ΔG^*_{solv} (exp)	Error
F^-	−78.3	3.0	−17.5	−92.8	−92.8	0.0
Cl^-	−58.4	4.5	−9.2	−63.1	−63.1	0.0
Br^-	−54.2	5.0	−10.7	−59.9	−59.9	0.0
I^-	−49.8	5.9	−7.6	−51.5	−55.0	+3.5
I_3^-	−38.6	14.0	−18.1	−42.7	−41.2	−1.5
N_3^-	−58.5	6.5	−10.0	−62.0	−62.1	+0.1
CN^-	−57.7	5.3	−5.8	−58.2	−58.0	−0.2
SCN^-	−50.0	7.7	−8.6	−50.9	−50.9	0.0
ClO_4^-	−50.9	9.4	−9.0	−50.5	−50.3	−0.2
$CH_3CO_2^-$	−58.6	9.8	−12.8	−61.6	−61.5	−0.1
Pic^-	−41.5	23.0	−22.8	−41.3	−41.5	+0.2
Mean absolute error						0.5
Mean error						0.2
SD						1.2

and a standard deviation of 1.2 kcal/mol, when we compare the results to the respective experimental data.

From Fig. 8 and Table 12, it becomes evident that the largest deviation between calculated and experimental ΔG^*_{solv} in AN occurs for the anions I^-, I_3^-, and ClO_4^-. The results obtained for the anions in DMF, displayed in Table 13 and Fig. 9, we observe only one larger deviation from experimental value in the case of the I^- anion, for which the theoretical free solvation energy is 3.5 kcal/mol larger than the experimental value.

It is worth to discuss the relative magnitude of the three contributions to the solvation free energy of the set of anions in AN and DMF solutions. In Methodology II, we are considering that the structural aspects related to the organization of the solvent molecules around a given anion are similar for all the solutes of the set solvated in AN or DMF. Based on this assumption, we applied a unique solvent dependent scaling factor to the atomic radii

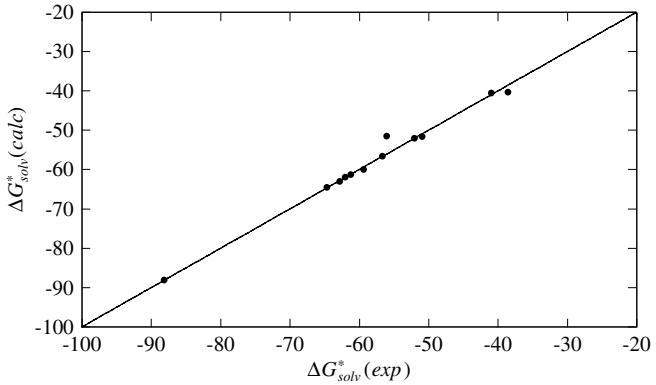

Fig. 8. Correlation of calculated ΔG^*_{solv}(calc) and experimental ΔG^*_{solv}(exp) free energies of solvation (in kcal/mol) for the set of anions in AN, using the approach including the steric terms in the computation of the solvation free energies.

of the solutes in the creation of the cavities. With the scaling factors defined for the solvation of anions in each solvent, and using the other physical parameters for the solvent required in the PCM, we computed the electrostatic and cavitation terms of the Gibbs free energies of solvation for the anions in AN and DMF. Thus, the procedures of parameterization for the PCM in Methodology II, have been reduced to the optimization of the parameters that relate the van der Waals term with the solvent exposed surface of each atom present in the solute. The possibility of performing an individual analysis of the contributions to the Gibbs free energies of the anions in AN or DMF is one of the greatest motivations for theoretical studies of anion solvation.

In the solvation of the F^- anion in AN, the theoretical results for the Gibbs free energy of solvation show that 93.5% of this energy stems from the electrostatic contribution. The van der Waals energy term contributes to the energy of solvation with 11.6%. In the solvent DMF, the electrostatic contribution represents 84.4% of the solvation energy and the steric terms correspond to 15.6%. The van der Waals energy represents 18.8% of the total free energy of F^- solvation in DMF. The cavitation energy term has a

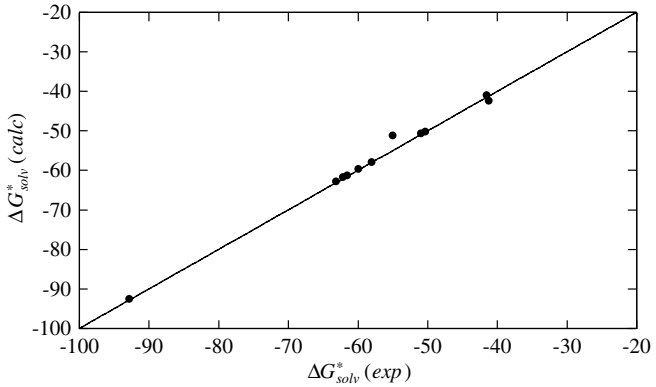

Fig. 9. Same as in Fig. 8, but for the solvation in DMF.

small positive contribution for the solvation of F^- anion in the two solvents studied. This term depends strongly on the solute size which in this case is the smallest of the solutes in the anion set and, therefore, the cavitation work is expected to be the smallest of all the studied anions. This observation confirmed by our data in both solvents is important to verify the consistency of the obtained values for the cavitation energy for all the solutes in this study.

In the case of F^- anion, the computed free energy of solvation becomes equal to the experimental value with an appropriate choice of the van der Waals atomic coefficient. The F^- anion is the only solute in the parameterized set of anions containing the fluorine atom in its structure. Thus, there is no statistical contribution of other solutes in determining the van der Waals parameter for this atom. The van der Waals parameter ξ_i for the fluorine atom is optimized as a free variable in the multiple linear regression procedure used in this methodology.

The results obtained for the Cl^- anion are interesting because the chlorine atom is also present in the ClO_4^- anion and, therefore, the van der Waals parameter optimized for the Cl atom is shared by more than one solute in the set. Thus, we are able to check the internal consistency of the parameters used to describe the van der Waals energy component in more than one solute in the set. We also are able to verify the quality of our methodology in modeling the solvation of different ions containing the same atoms. Our results for the Cl^- anion indicate that this simple methodology produces excellent accordance with the experimental values for the energies of solvation in AN and DMF. For the solvation of the Cl^- anion in AN, we computed a free energy of solvation of -64.4 kcal/mol. This value is only 0.1 kcal/mol larger than the experimental value. In DMF solution, the energy of solvation calculated for the Cl^- anion is -63.1 kcal/mol, in perfect agreement with the experimental energy of solvation. Comparing the individual terms of the Gibbs free energy of solvation (ΔG_{ele}, ΔG_{cav} and ΔG_{vdW}) for the Cl^- anion in AN and DMF, we note that the largest contribution stems from the electrostatic term representing more than 90% of the total energy of solvation. 4.2% of the solvation energy for the Cl^- anion in AN is due to the steric contribution ($\Delta G_{cav} + \Delta G_{vdW}$) increased in DMF solution to 7.5%. Thus, we can confirm the assumption employed in the first proposal of parameterization (Methodology I) that the process of solvation of ions is dominated by the electrostatic energy of interaction of the ion with the solvent molecules.

We observe a similar pattern in the solvation of the Br^- anion. In the solvation of this ion in AN, 93.1% of the Gibbs free energy of solvation is electrostatic. In DMF, the electrostatic energy contributes as much as 90.5% to the total energy of solvation for this anion. As in the F^- case, the Br^- is the only anion in our set that contains the bromine atom. Thus, the van der Waals parameter for the bromine anion has been chosen to yield perfect agreement between theory and experiment.

In the case of the iodine atom, we have again an example for the presence of the same atom in two different solutes within the parameterization set (I^- and I_3^-). The I_3^- anion as a non-spherical solute differs from the ideal spherical symmetry of the halide anions that were utilized to determine the scaling factor for the creation of the cavities for all the solutes in the set. Thus, the calculation of the energy of solvation for the I_3^- anion represents an opportunity to verify the accuracy of this methodology applied to solutes which request molecular cavities of more complex geometries.

The Gibbs free energy of solvation calculated for the I^- anion in AN exhibits a deviation of 4.5 kcal/mol and, for solvation in DMF, we notice a deviation of 3.5 kcal/mol from the experimental data. These are the largest errors found in our results within the application of Methodology II. For the I_3^- anion, we observe similar pattern in the distribution of steric and electrostatic contributions to the total free energy of solvation as we observe for the halide anions. The electrostatic energy is the most important contribution. The deviations in the results for the I_3^- anion in AN are -1.8 kcal/mol and -1.5 kcal/mol in DMF. To comment these results, it is worth to mention that the I_3^- anion represents a hydrophobic ion, as indicated by the negative free Gibbs energies of transfer in Table 1. The computed free energies of solvation reproduce the experimental observation that the Gibbs free energy of solvation for the I_3^- anion is more negative in the organic solvents than in water (-34.8 kcal/mol). Thus, our Methodology II is capable to include the hydrophobic character of anions. However, as the deviations in the theoretical results point into the negative direction, our model overestimates slightly the affinity of the I_3^- anion to the organic solvents by a few kcal/mol.

For the I^- anion, Table 1 furnishes positive Gibbs free energies of transfer of 4.0 kcal/mol for AN and 4.9 kcal/mol for DMF. For this anion, we have noticed the strongest deviation between our model and experiment surpassing in the case of solvation in AN the transfer free energy from water. However, the important fact here is the sign of the errors. In both solvents, AN and DMF, the results obtained for the free energies of solvation for the I^- anion are less negative than the experimental data. Thus, our Methodology II correctly includes the process of transferring I^- anions from water to the organic solvents AN and DMF, at least as a qualitative measure. Our data correctly confirm that the energy of solvation in the organic phase is less negative than in the aqueous phase, although quantitatively the IEF-PCM results in the present study overestimate the increase in the Gibbs free energy of solvation for I^- in the solvents AN and DMF.

Combining our results for the I^- and I_3^- anions suggests that it is possible to describe the solvation of non-spherical anions by the same set of parameters that have been determined via MD simulations of the solutions containing the simple halide anions in AN and DMF. Although the scaling factor for radii has been estimated from studies on the

structure of the solvated spherical solutes, the results demonstrate that the information obtained about the structure of the first solvation shell may be extended to cases of solutes with more complex molecular geometries. This statement is based only on the internal consistency of the our results obtained for the energies of solvation for this set of solutes. In order generalize our conclusion, more detailed studies on the structure of solutions of ions in AN and DMF are necessary.

A possible explanation for the deviations observed in the computed energies of solvation for the solutes containing the iodine atom, especially for the I^- anion, is the fact that our methodology for the determination of the van der Waals parameters follows an ideal behavior in which a single van der Waals parameter ξ_I is assumed to model the van der Waals interaction for I^- and I_3^-. One might expect that the iodine atoms in these solutes experience different environments resulting in different van der Waals parameters. However, the undertaken assumptions are necessary to get satisfactory results in a theoretical model for the solvation using as few parameters as possible. This concept applied to the solvation of anions might also be justified by the fact that van der Waals terms in ΔG^*_{solv} are not the most important contributions. We note that the thermodynamics of solvation for the I^- and I_3^- anions in AN or in DMF solutions is better described by our Methodology I (with deviations less than 0.8 kcal/mol in both solvents) that considers the electrostatic term as the only energy of solvation.

The results for the Gibbs free energy of solvation for the N_3^- anion in AN and DMF present (deviations of 0.1 kcal/mol in both solvents) excellent agreement with experimental energies of solvation. As the nitrogen atom is present in five different solutes in AN and four solutes in DMF, we conclude that Methodology II works very well for the solutes containing nitrogen atoms in their structures. The analysis of the partial contributions to the solvation energy for the N_3^- anion follows the profile of the halide anions. The electrostatic energy contributes with 97.1% to the solvation energy in AN and 94.3% in DMF. The van der Waals energy represents 15.5% of the total energy in AN and 16.2% of the energy of solvation in DMF. The cavitation energy for the N_3^- anion is comparable with that for the I^- anion.

The CN^- anion is an important anion for studies on chemical reactivity. Its solvation in AN and DMF is also dominated by the electrostatic component representing almost 100% of the solvation free energy. The cavitational and van der Waals energies possess opposite signs, giving as a sum, an insignificant contribution to the total energy of solvation for this anion. The deviation in the Gibbs free energy of solvation for the CN^- anion from the experimental energy is only −0.6 kcal/mol in AN and −0.2 kcal/mol in DMF. For this anion, the uncertainty in the experimental value is approximately ±1.7 kcal/mol [31,59]. The theoretical results are within this range and support the consistency of the methodology reported here.

At a first glance, the computed free energies of solvation for the SCN^- anion in AN and DMF correspond to the electrostatic solvation energy. In the first part of this study, where we described solvation by a purely electrostatic term, we observed that the Gibbs free energy of solvation for the SCN^- anion is not well represented by that simplified methodology, probably due to missing cavitational contributions for this anion. Applying Methodology II, we conclude that the larger cavity for the solute accompanied by the inclusion of the steric contributions to the energy of solvation improves the theoretical result.

The NO_3^- anion is only present in the set of solutes for the AN solvent. We found no deviation between calculated and experimental free energy of solvation. Considering that oxygen and nitrogen atoms are also present in other anions, again, we were able to verify the consistency of Methodology II.

The free energy of solvation computed for the ClO_4^- anion using Methodology II is −51.5 kcal/mol in AN and −50.5 kcal/mol in DMF solution. The calculated energy of solvation for the ClO_4^- anion in DMF is −0.2 kcal/mol lower than the experimental value, whereas the difference between the calculated and the experimental values of the energy of solvation in AN is only −0.7 kcal/mol. This good agreement with experimental data for the ClO_4^- anion is very important for two reasons. Firstly, it represents another positive test for the general applicability of Methodology II working very well for the two solutes containing the chlorine atom in their structures, the Cl^- and the ClO_4^- anions. For these two anions, it was possible to calculate the exact energy of solvation in DMF. In AN solutions, the results are within the range of experimental uncertainty. The second important aspect in the agreement of experimental and theoretical data for the perchlorate is that these results help to solve the controversies about the real experimental value for the Gibbs free energies of solvation for the ClO_4^- anion in AN and DMF. The Gibbs free energies of solvation computed by the application of Methodology II support the experimental data reported by Abraham and Liszi [37].

For the $CH_3CO_2^-$ anion, we computed a Gibbs free energy of solvation in AN that is only 0.2 kcal/mol lower than the experimental value. And in DMF solution, the calculated free energy is equal to the experimental measure. Thus, we achieved excellent accordance with the experimental data. The range of uncertainty for the experimental value in AN is ±4.0 kcal/mol [31,59]. The Gibbs free energy of transfer for the $CH_3CO_2^-$ anion between water and the solvents AN and DMF is approximately 15 kcal/mol (Table 1). Therefore, with the accuracy of the results obtained in the present work, it would be possible to calculate the change in the free energy of the $CH_3CO_2^-$ solute when it is transferred from water to one of these solvents. These results are also relevant due to the broad application of the $CH_3CO_2^-$ anion appearing in several chemical processes. If we analyze the individual terms of the Gibbs free energy of solvation for the $CH_3CO_2^-$ anion, we note that

the contributions from cavitation and van der Waals energies represent 3% of the total energy in AN and 4.7% of the total energy of solvation in DMF. Thus, although this anion is bigger and possessing a more complex structure than other anions, it follows the general trend in free energy partitioning that we observed for the smaller and simpler solutes like Cl^- and N_3^-.

Finally, we describe our results for the picrate anion. This is one of the most important anions from the point of view of this theoretical study of anion solvation in AN and DMF. It possesses 18 atoms from four different elements (H, C, N, and O). Therefore, it represents the most rigorous test for the quality, consistency, and capability of our Methodology II to model the solvation of anions. If this methodology is able to produce accurate results for the Gibbs free energy of solvation of the Pic^- anion, then we believe that we are also enable to compute accurate results for the class of anions derived from phenols and benzoic acid with similar structures and charge distributions.

As one might expect from the molecular properties of the Pic^- anion, the inclusion of the steric terms is important in modeling correctly the solvation of this anion. In the solvation of the Pic^- anion in AN, the cavitation energy added to the van der Waals energy is equal to 2.4 kcal/mol. So the steric terms contribute to the Gibbs free energy of solvation in AN with a positive value. This means that the cavitation contribution overcomes the contribution stemming from the van der Waals energy. In the solvation of the Pic^- anion in DMF, the cavitation energy is also larger than the van der Waals energy. The steric contributions for the solvation of Pic^- in DMF add up to 0.2 kcal/mol. We note that in this case the experimental Gibbs free energy of solvation is exactly reproduced by the calculated electrostatic contribution to the energy of solvation. When we compare the computed free energy of solvation for the Pic^- anion in AN with the experimental value, we find a deviation of 0.4 kcal/mol. And the energy of solvation computed for this ion in AN is 0.6 kcal/mol lower than the hydration energy, in agreement with the fact that this anion is better solvated in organic solvents as evidenced by the negative values for the Gibbs free energies of transfer from water to AN or DMF (Table 1). Thus, our results attest the efficiency of Methodology II in producing accurate results for the Gibbs free energies of solvation of several kinds of anions containing different atom types arranged in different molecular structures. In the Pic^- case, we have four different atom types which are also present in five other solutes in the set. The combination of the parameters optimized for the computation of the van der Waals energy added to the cavitation energy and the electrostatic term is able to produce accurate results for the free energies for all these anions in AN and DMF. It is important to note that although we are using a continuum model to represent the solvent properties, the differences in the parameters obtained for describing the solutes in the two solvents are able to mimic the real physical differences in the electrostatic and non-electrostatic interactions between the anions and the solvent molecules.

4. Conclusions

We have presented the parameterization of the PCM for the solvation of monovalent anions in AN and DMF. The optimization of the molecular cavity size based on the approach which considers the solvation energy as a pure electrostatic term has furnished a scaling factor for the solute's atomic radii of 1.36 for anions in AN and of 1.39 for anions in DMF. In the parameterization aided by MD simulations, we included the cavitation energy and also parameterized the van der Waals parameters. In this second approach of parameterization, we obtained the scaling factors of 1.44 and 1.52 for the solvation in AN and DMF, respectively.

The comparison of free energies of solvation from the two methodologies show that, for most of the anions in the investigated set, it is a good approximation to consider only the electrostatic term. The smaller effective scaling factors obtained from Methodology I reduce naturally steric contributions. The parameterization procedure includes anions of different sizes (up to 18 atoms) containing several atom types. The optimized model has been applied to the calculation of the solvation Gibbs free energies for 13 anions in AN and twelve anions in DMF. Larger deviations observed in the calculations were explained by the neglect of some molecular interactions in the theoretical approach, but also by experimental problems in the determination of thermodynamic quantities of transfer. When the cavitation and van der Waals terms are included in the parameterization, most of the deviations in the results are removed.

The present and similar studies are important for revising some problems related to the determination of the thermodynamics describing ion solvation and ion transfer from water to organic solvents. The parameterized model allows us to calculate, with accuracy, solvation energies for anions in organic solvents that combined with the corresponding data for water promise an estimate for energies of transfer between water and the organic solvents. In addition, the optimized model also represent anion–solvent interactions for the study of chemical reactions and other operations performed in AN or DMF solutions.

Acknowledgement

We gratefully appreciate stimulating discussions with Dr. Paulo F.B. Gonçalves and his valuable advice for the realization of the present study.

References

[1] R. Alexander, E.C.F. Ko, A.J. Parker, T.J. Broxton, J. Am. Chem. Soc. 90 (1968) 5049.
[2] W.L. Dilling, J. Org. Chem. 31 (1966) 1045.
[3] C.N.R. Rao, S. Singh, V.P. Senthilnathan, Chem. Soc. Rev. 5 (1976) 297.
[4] C. Reichardt, Solvents and Solvent Effects in Organic Chemistry, VCH, New York, 1990.

[5] A.J. Parker, Chem. Rev. 69 (1969) 1.
[6] J. Miller, A.J. Parker, J. Am. Chem. Soc. 83 (1961) 117.
[7] M. Allen, D.J. Tildesley, Computer Simulations of Liquids, Clarendon, Oxford, 1987.
[8] A. Pullman, B. Pullman, Q. Rev. Biophys. 7 (1975) 505.
[9] J. Tomasi, M. Persico, Chem. Rev. 94 (1994) 2027.
[10] J. Tomasi, B. Mennucci, R. Cammi, Chem. Rev. 105 (2005) 2999.
[11] C.J. Cramer, D.G. Truhlar, Chem. Rev. 99 (1999) 2161.
[12] P.F.B. Gonçalves, H. Stassen, J. Comput. Chem. 23 (2001) 706.
[13] P.F.B. Gonçalves, H. Stassen, J. Comput. Chem. 24 (2003) 1758.
[14] P.F.B. Gonçalves, H. Stassen, Pure Appl. Chem. 76 (2004) 231.
[15] P.F.B. Gonçalves, H. Stassen, J. Chem. Phys. 123 (2005) 214109.
[16] F.J. Luque, M.J. Negre, M. Orozco, J. Phys. Chem. 97 (1993) 4386.
[17] S. Miertus, E. Scrocco, J. Tomasi, Chem. Phys. 55 (1981) 177.
[18] S. Miertus, J. Tomasi, Chem. Phys. 65 (1982) 239.
[19] J.L. Pascual-Ahuir, E. Silla, J. Tomasi, R. Bonaccorsi, J. Comput. Chem. 8 (1987) 778.
[20] E. Cances, B. Mennucci, J. Tomasi, J. Chem. Phys. 107 (1997) 3032.
[21] E. Cances, B. Mennucci, J. Math. Chem. 23 (1998) 309.
[22] M. Orozco, F.J. Luque, Chem. Rev. 100 (2000) 4187.
[23] F.J. Luque, C. Curutchet, J. Muñoz-Muriedas, A. Bidon-Chanal, I. Soteras, A. Morreale, J.L. Gelpí, M. Orozco, Phys. Chem. Chem. Phys. 5 (2003) 3827.
[24] F.J. Luque, Y. Zhang, C. Alemán, M. Bachs, J. Gao, M. Orozco, J. Phys. Chem. 100 (1996) 4269.
[25] F.J. Luque, C. Alemán, M. Bachs, M. Orozco, J. Comput. Chem. 17 (1996) 806.
[26] C. Curutchet, M. Orozco, F.J. Luque, J. Comput. Chem. 22 (2001) 1180.
[27] M. Orozco, F.J. Luque, Chem. Phys. 182 (1994) 237.
[28] C. Curutchet, A. Bidon-Chanal, I. Soteras, M. Orozco, F.J. Luque, J. Phys. Chem. B 109 (2005) 3565.
[29] J.R. Pliego Jr., J.M. Riveros, Chem. Phys. Lett. 355 (2002) 543.
[30] K. Weissermel, H.J. Arpe, Industrial Organic Chemistry, VCH, Weinheim, 1993.
[31] Y. Marcus, Pure Appl. Chem. 55 (1983) 977.
[32] Y. Marcus, Pure Appl. Chem. 57 (1985) 1103.
[33] J.R. Pliego Jr., J.M. Riveros, Phys. Chem. Chem. Phys. 4 (2002) 1622.
[34] Y. Marcus, Biophys. Chem. 51 (1994) 2995.
[35] J. Florian, A. Warshel, J. Phys. Chem. B 101 (1997) 5583.
[36] S. Kusakabe, M. Arai, Bull. Chem. Soc. Jpn. 69 (1996) 581.
[37] M.H. Abraham, J. Liszi, J. Chem. Soc. Faraday Trans. 74 (1978) 1604.
[38] M.D. Tissandier, K.A. Cowen, W.Y. Feng, E. Gundlach, M.H. Cohen, A.D. Earhart, J.V. Coe, T.R. Tuttle, J. Phys. Chem. A 102 (1998) 7787.
[39] A. Ben-Naim, J. Phys. Chem. 82 (1978) 792.
[40] D.M. Camaioni, C.A. Schwerdtfeger, J. Phys. Chem. A 109 (2005) 10795.
[41] A. Ben-Naim, Y. Marcus, J. Chem. Phys. 81 (1984) 2016.
[42] M.W. Schmidt, K.K. Baldridge, J.A. Boatz, S.T. Elbert, M.S. Gordon, J.H. Jensen, S. Koseki, N. Matsunaga, K.A. Nguyen, S.J. Su, T.L. Windus, M. Dupuis, J.A. Montgomery, J. Comput. Chem. 14 (1993) 1347.
[43] C. Colominas, F.J. Luque, J. Teixidó, M. Orozco, Chem. Phys. 240 (1999) 253.
[44] M. Cossi, B. Mennucci, R. Cammi, J. Comput. Chem. 17 (1996) 57.
[45] B. Mennucci, J. Tomasi, J. Chem. Phys. 106 (1996) 5151.
[46] J. Emsley, The Elements, Clarendon Press, Oxford, 1991.
[47] J.A. Riddick, W.B. Bunger, Organic Solvents Physical Properties and Methods of Purification, John Wiley & Sons, New York, 1986.
[48] A.P. Lyubartsev, A. Laaksonen, Comput. Phys. Comm. 128 (2000) 565.
[49] N.A. McDonald, E.M. Duffy, W.L. Jorgensen, C.J. Swenson, J. Am. Chem. Soc. 120 (1998) 5104.
[50] D.M.F. Edwards, P.A. Madden, I.R. McDonald, Mol. Phys. 51 (1984) 1141.
[51] W.L. Jorgensen, C.J. Swenson, J. Am. Chem. Soc. 107 (1985) 569.
[52] P. Ewald, Ann. Phys. 64 (1921) 253.
[53] M. Tuckerman, B.J. Berne, J. Chem. Phys. 97 (1992) 1990.
[54] S. Nosé, Mol. Phys. 23 (1984) 327.
[55] J.P. Ryckaert, G. Ciccotti, H.J.C. Berendsen, J. Comput. Phys. 23 (1977) 327.
[56] R.A. Pierotti, Chem. Rev. 76 (1976) 717.
[57] P. Claverie, in: B. Pullman (Ed.), Intermolecular Interactions: From Diatomics to Biomolecules, Wiley, Chichester, 1978.
[58] D.C. Montgomery, G.C. Runger, Applied Statistics and Probability for Engineers, John Wiley & Sons, New York, 1999.
[59] J.R. Pliego Jr., J.M. Riveros, Chem. Phys. Lett. 332 (2000) 597.
[60] Y. Marcus, J. Chem. Soc. Faraday Trans. 87 (1991) 2995.
[61] E.A. Gomaa, Thermochim. Acta 142 (1989) 19.
[62] R. Gulaboski, V. Mirčeski, F. Scholz, Electrochem. Commun. 4 (2002) 277.
[63] Y. Marcus, Electrochim. Acta 44 (1998) 91.
[64] Y. Marcus, Z. Naturforsch. A 50 (1995) 51.
[65] J.S. Loring, W.R. Fawcett, J. Phys. Chem. A 103 (1999) 3608.
[66] D.W. James, R.E. Mayes, J. Phys. Chem. 88 (1984) 637.
[67] J. Barthel, K. Bachhuber, R. Buchner, Z. Naturforsch. A 50 (1995) 65.
[68] T. Osakai, A. Ogata, K. Ebina, J. Phys. Chem. B 101 (1997) 8341.
[69] C. Tanford, The Hydrophobic Effect: Formation of Micelles and Biological Membranes, John Wiley, New York, 1980.
[70] F.M. Floris, J. Tomasi, J.L. Pascual-Ahuir, J. Comput. Chem. 12 (1991) 784.
[71] A. Morreale, J.L. Gelpí, F.J. Luque, M. Orozco, J. Comput. Chem. 24 (2003) 1610.
[72] G.D. Hawkins, C.J. Cramer, D.G. Truhlar, J. Phys. Chem. B 102 (1998) 3257.
[73] M. Born, Z. Phys. 1 (1920) 45.
[74] J. Bockris, A.K.N. ReddyModern Electrochemistry: An Interdisciplinary Area, vol. 1, Plenum, New York, 1973.
[75] C.S. Babu, C.L. Lim, Chem. Phys. Lett. 310 (1999) 225.
[76] D.R. Lide, CRC Handbook of Chemistry and Physics, CRC Press, Boca Raton, 1995.
[77] V. Renugopalakrishnan, G. Madrid, G. Cuevas, A.T. Hagler, Proc. Indian Acad. Sci. (Chem. Sci.) 112 (2000) 35.
[78] T.V. Nguyen, G.H. Peslherbe, J. Phys. Chem. A 107 (2003) 1540.
[79] R. Ayala, J.M. Martinez, R.R. Pappalardo, E.S. Marcos, J. Phys. Chem. A 104 (2000) 2799.
[80] G. Grégoire, V. Brenner, P. Millié, J. Phys. Chem. A 104 (2000) 5204.
[81] D.D. Kemp, M.S. Gordon, J. Phys. Chem. A 109 (2005) 7688.
[82] Z.M. Loh, R.L. Wilson, D.A. Wild, E.J. Bieske, M.S. Gordon, J. Phys. Chem. A 109 (2005) 8481.